Journal of Materials Science and Engineering B 4 (4) (2014) 95-108

Preparation and Characterization of Copper Borates as Lubricant Additives

Burcu Alp, Sevdiye Atakul Savrik and Devrim Balkose

Department of Chemical Engineering, İzmir Institute of Technology, Gülbahçe Urla Izmir 35430, Turkey

Received: April 05, 2014 / Accepted: April 17, 2014 / Published: April 25, 2014.

Abstract: The present study attempts the preparation of copper borate as a lubricating oil additive by the reaction of copper nitrate and borax solutions. Effects of borax/ copper ratio, surface active agent (Span 60), pH, temperature and mixing time on properties of the products were investigated. The obtained products were not pure form; therefore they were analyzed in detail. They were characterized by color measurement, X-ray diffraction, SEM, zeta sizer, ICP, EDX, TG, DSC, CHNS analysis and FTIR spectroscopy. Mainly $Cu_2(OH)_3NO_3$ with nitrate ions partially substituted with borate ions was obtained at pH 3.7. There were borate ions equivalent to 0.32 mols of $Cu(BO)_2$ per mol of $Cu_2(OH)_3NO_3$. The borate ions should have replaced partially the nitrate ions in $Cu_2(OH)_3NO_3$ without changing its crystal structure. On the other hand, $Cu(BO_2)_{1.5}(OH)_{0.74}\cdot(H_2O)_{0.15}$ was produced at pH 10.2. It also contained 0.11 mol NO_3^- per mol. By mixing of dilute solutions at pH 8.2 and drying at room temperature nanoparticles of $Cu(BO_2)_{1.5}(H_2O)_6$ having 0.05 NO_3^- per mol was obtained. The precipitates obtained at pH 10.1 and 8.2 were tested as lubricant additives. When they were added to lubricating oil with Span 60, the friction coefficient was reduced 28 % and 65 % for the precipitates prepared at pH 10.1 and 8.2, respectively.

Key words: Copper borate, copper hydroxyl nitrate, lubricant additive, characterization.

1. Introduction

The materials showing antiwear and extreme pressure functions and used for the modification of the surfaces in the lubricating oils can be borate based material [1]. Copper borate has been the focus of much attention, as it possesses a good combination of properties, such as environmentally friendly lubrication, wood preservation, and fire retardancy. Hydrophobic copper borate particles captured attention as a solid lubricant since it reduced the friction coefficient of the base oil [2]. 1% hydrophobic copper borate particles in mineral oil reduced the friction coefficient of the base oil from 0.116 to 0.012. Moreover copper nanoparticles dispersed in base oil also improved lubrication behavior. The wear scar diameter and the friction coefficient were reduced 16% and 8% respectively at 80 °C. Local high temperature and high pressure due to direct contact of two surfaces initiate melting of Cu nanoparticles and forming a copper protective film with low nano-hardness and elastic modulus of worn surface [3].

Hu et al. [1], Zheng et al. [2] and Shvartz and Boleuseva [4, 5] described the preparation of copper borate from borax decahydrate and water soluble copper salts. Formation of $Cu_3B_2O_6$ [1], $CuBO_2$ [2] and $2CuO\cdot3B_2O_3\cdot nH_2O\cdot mNa_2SO_4$ [4] were reported by mixing aqueous solutions of copper salts and borax decahydrate. The conditions under which tricuprotetraborate hexahydrate $3CuO.2B_2O_3.6H_2O$ was formed were as follows: $CuSO_4$:H_3BO_3:NaOH 1:4:(3.25-3.5), pH 7.5-8.0, 80 °C [5]. The synthesis duration was 4 h. Under other conditions, amorphous finely dispersed tricuprotetraborate with a significant amount of impurities (Na_2SO_4, $Cu(OH)_2$, etc.) was

Corresponding author: Devrim Balkose, Dr., professor, research fields: polymer composites, additives to polymers and lubricants and water material interactions. E-mail: devrimbalkose@gmail.com.

formed [5].

$Cu_3B_6O_{12}·H_2O$ was synthesized by heating cupric oxide and boric acid at 700 °C and at 7.5 GPa [6]. The crystals were built up from corner sharing of BO_4 tetrahedra forming a three dimensional network with channels along c-axis. Inside these channels, the water molecules and a part of the copper ions took place.

There are parallel reactions that could occur in the mixtures of aqueous copper nitrate and sodium borate solutions. The basic borate solutions may lead to the formation of copper hydroxy nitrate besides copper borate. Conventionally, copper hydroxy nitrate is synthesized by mixing aqueous solutions of copper nitrate and sodium carbonate [7]. Depending on the ratio of the reactants different copper hydroxy nitrates can be formed. They are $Cu_2NO_3(OH)_3$, $CuNO_3OH$, $Cu_3(NO_3)(OH)_5·2H_2O$ and $Cu_3(NO_3)_2(OH)_4$ [7]. $Cu_2(OH)_3NO_3$ was also obtained by mixing aqueous $Mg(OH)_2$ dispersions with copper nitrate solutions [8]. Another method was the addition of ammonia solution to copper nitrate solution [9]. Heating hydrated copper nitrate above 140 °C was an alternative method to synthesize copper hydroxy nitrate [10]. Mixing dilute copper nitrate and sodium hydroxide solutions in a jet is a convenient method to produce nanoplatelets [11].

$Cu_2(OH)_3NO_3$ was used as a raw material for other products . The $Cu(OH)_2$ nanorods were prepared from direct reaction of $Cu_2(OH)_3NO_3$ with aqueous NaOH solution at room temperature [12]. Other salts were prepared from $Cu_2(OH)_3NO_3$ by anion exchange of nitrate ions [10, 13]. Partial substitution of nitrate ions by benzoate ions was possible by mixing copper hydroxynitrate with aqueous sodium benzoate solution at 25 °C for 24 h and coordination of carboxylic acid groups were bidendate in structure [10]. Perclorate ions were substituted with nitrate ions of copper hydroxy nitrate mixed with aqueous sodium perchlorate solution in eight days [14]. Copper hydroxydodecyl sulfate was obtained by substituting the nitrate ions in $Cu_2(OH)_3NO_3$ with the dodecyl sulfate ions. The distance between the layers was expanded due to introduction of dodecyl sulfate between the layers [9].

The present study aims at preparation of nanosized copper borate particles by mixing copper nitrate and borax solutions. The effects of concentration of reactants, surface active agent (Span 60) additive, pH, temperature and mixing time on chemical composition and morphology of the products were investigated. The products were characterized by color measurement, SEM, zetasizer, X-ray diffraction, FTIR spectroscopy, thermal gravimetric analysis, differential scanning calorimetry, inductively coupled plasma, EDX and CHNS analysis. The products were used as an additive to a lubricating oil to improve its tribological properties.

2. Experiments

2.1 Precipitation Reaction

Copper (II) nitrate, $Cu(NO_3)_2·2.5H_2O$ (from Aldrich), borax decahydrate, $Na_2B_4O_7·10H_2O$ (from Etibor with purity 99%) and NaOH (from Merck) were used in preparation of copper borates. Sorbitan monostearate (Span 60, from Aldrich) (0.02 $mol·dm^{-3}$) was used as a surface active agent. 0.1-2.5 $mol·dm^{-3}$ Copper (II) nitrate and 0.1-1 $mol·dm^{-3}$ borax decahydrate solutions having different concentrations were mixed in proportions shown in Table 1 to prepare copper borates. Mainly there different methods were used in preparation of the precipitates. The concentrations and proportions of the Method 1 and Method 2 were inspired from Zheng et al. [2] and Shvartz and Belousova [4, 5] previous studies, respectively. Copper nitrate was used in the present study instead of copper sulfate used in previous studies. As surface active agent Span 60 was used instead of the phosphate ester used by Zheng et al. [2]. Dilute $Cu(NO_3)_2$ and borax solutions were mixed 25 °C to prevent particle growth and agglomeration and to obtain nano sized copper borate particles in Method 3. Copper (II) solutions were added drop by drop to borax solutions which were stirred at 450 rpm using a magnetic stirrer.

Table 1 Experimental composition, pH, temperature and mixing period.

Method	Borax solution ($mol \cdot dm^{-3}$)	Copper Solution ($mol \cdot dm^{-3}$)	Borax/Copper (mol/mol)	NaOH/Copper (mol/mol)	Final Span 60 concentration (10^5 $mol \cdot dm^{-3}$)	pH	Temperature (°C)	Time (h)
1	0.1	2	0.25	0	0	3.7	40-70	2-4
1	0.1	2	0.25	0	3.3	3.7	40-70	2-4
2	0.3	2.5	0.85	2.88	0	10.1	60	3
3	0.1	0.1	1.0	0	0	8.2	25	2
3	0.1	0.1	1.0	0	2	8.2	25	2

Since the copper nitrate solutions are acidic and borax solutions are basic their mixtures had a pH value depending on their proportions. For example when 0.1 $mol \cdot dm^{-3}$ $Cu(NO_3)_2$ solution and 0.1 $mol \cdot dm^{-3}$ borax solution were mixed in equimolar quantities the final pH value was 8.2. Thus mixtures with different final pH values were obtained by changing the mol ratio of borax to copper or by adding 1 $mol \cdot dm^{-3}$ NaOH solution. The final pH of the mixtures were measured and the obtained precipitates were filtered, washed with water twice and then dried for 2 h at 60 °C in the air circulating oven.

2.2 Characterization of the Precipitates

The colors of the precipitates were measured by using Avantes AvaMouse Fiberoptic spectrophotometer. The morphologies of the samples were examined using QUANTA 250F Scanning Electron Microscope (SEM). The particle size of the powders were measured by Malvern 2000 zetasizer. X-ray diffraction diagrams were obtained by Phillips x'pert pro x-ray diffractometer employing Ni-filtered Cu K_α radiation. FTIR spectra of the samples were taken with SHIMADZU FTIR-8400S using KBr disc technique. TG analysis was performed by using SHIMADZU TGA-51 to determine changes in weight with heating under nitrogen flow at 40 $cm^3 \cdot min^{-1}$ rate and at a heating rate of 10 °C·min^{-1} up to 600 °C. DSC analysis was carried out using SHIMADZU DSC-50 by heating the samples under 40 cm^3min nitrogen flow and at a heating rate of 10 °C·min^{-1} up to 600 °C. Thermal decomposition behavior of the product was studied by *in situ* temperature-programmed diffuse reflectance Fourier transform infrared spectroscopy (DRIFTS) method using a FTS 3000MX Digilab Excalibur Series spectrophotometer. The samples were heated in situ from the room temperature up to 500 °C at a heating rate of 2 °C/min under vacuum (0.1 Pa) in a praying mantis diffuse reflection attachment (Harrick Scientific Products Inc.) equipped with a high-temperature, low-pressure reaction chamber (HVC-DRP, Harrick Scientific Products Inc.). The reaction chamber has two CaF_2 windows and one glass window for observation. The pressure in the chamber was controlled with Leybold PT50 Vacuum system.

The copper content of the samples were determined using an inductively coupled plasma atomic emission spectrometer with axial plasma (ICP-AES) (Liberty Series II, Varian) after dissolving them in nitric acid. Boron content was determined by adding mannitol after masking copper ions with ethylene diamine tetra acetic acid (EDTA) at pH 9 and titrating released protons with NaOH. EDX analysis was carried out using QUANTA 250F SEM. Besides, elemental analysis of the samples was performed using CHNS Analyzer (LECO Corporation St. Joseph MI USA).

2.3 Lubricant Preparation and Characterization

The precipitates obtained by method 2 (pH 10.1) and method 3(without Span 60, pH 8.2) described in Table 1 were employed as lubricant additives to oil. In a typical experiment, 50 cm^3 of spindle oil (PETROFER A.Ş., Turkey), 0.5 g of sorbitan monostearate and 0.5 g of the precipitate were mixed thoroughly at 600 rpm rate and at 160 °C for one hour on a magnetic hot plate and left to cool down to room temperature by

continuous stirring. A four ball tester (Ducom) was used to determine the friction coefficient and wear scar diameter. The tests were performed according to ASTM D 4172-94 at 392 N and the test duration was 1 h at 75 °C. Test balls were made from AISI standard steel No. E-52100 and had 12.7 mm diameter.

Microphotographs of the wear scars of the three fixed and one rotating test balls were taken by using Olympus BX 60 equipped with Canon Power shot 590IS camera.

3. Results and Discussion

3.1 Colors of the Precipitates

The color of a substance can be defined by L, a and b coordinates. While the L value describe the lightness of the color, the values of a and b indicate the color falls along red-green axis, and yellow-blue axis, respectively. The positive and negative values of a represent redness and greenness of the color respectively. Positive values of "b" represents yellowness and negative values of "b" represents blueness of the color. Representative colors of the precipitates are seen in Fig. 1 and the L, a, and b values are listed in Table 2, as well. The precipitates obtained at pH 3.7 and 8.2 had the same blue color and L, a and b values as 73, -20 and -26.7, respectively. On the other hand L, a and b values of the precipitate obtained at pH 10.1 were 66, -17.9 and -3.3. The sample obtained at pH 10.1 was darker and less blue since it had a lower L value and a less negative b value than the color of the precipitates obtained by at pH 3.7 and 8.2.

3.2 Morphologies of the Precipitates

The particles formed in precipitation reaction at pH 3.7 are in planar geometry with average dimensions of 2 ± 0.2 μm length and 1 ± 0.1 μm width and 100 ± 10 nm thickness as seen in the representative SEM images of the samples prepared under different conditions (Figs. 2a and 2b). They were heavily intertwined with each other. The particles were larger in size but had the same morphology with the copper hydroxyl nitrate nanoplatelets prepared by previous investigators [11]. The morphologies of the precipitates formed at pH 3.7 but at different temperatures, mixing time periods and

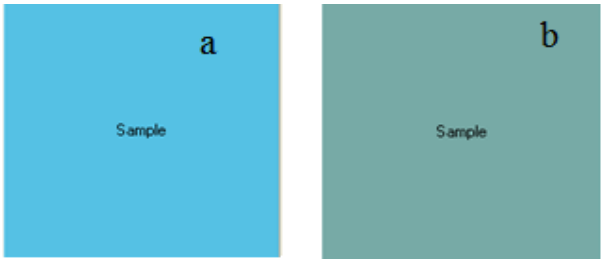

Fig. 1 The representative colors of the precipitates prepared at (a) pH 3.7 and (b) 8.2 10.1.

Table 2 L, a, b values of products.

Method	pH	L	a	b
1	3.7	73	-20	-26.7
2	10.1	66	-17.9	-3.3
3	8.2	73	-20	-26.7

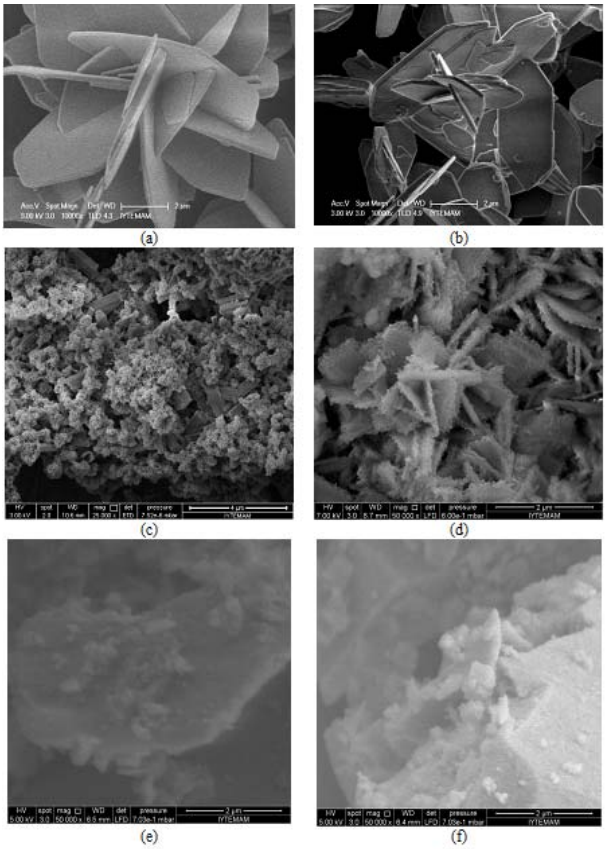

Fig. 2 SEM images of samples produced at (a) 70 °C and without Span 60 for 4 h at pH 3.7 (b) 70 °C and with Span 60 for 4 h at pH 3.7 (c) 60 °C, without Span 60 at pH 10.1 (scale 4 μm) (d) 60 °C, without span 60 at pH 10.1 (scale 2 μm) (e) 25 °C and without Span 60 at pH 8.2 (scale 2 μm) (c) 25 °C and with Span 60 at pH 8.2 (scale 2 μm).

in the presence and the absence of Span 60 at pH 3.7 were also very similar to each other as seen in Fig. S1. The morphologies of the particles did not change with temperature, time of mixing and presence of Span 60 during preparation.

There are two different types of particles in the precipitate formed in at pH 10.1 as seen in Figs. 2c and 2d. Prismatic particles with 2 μm × 0.25 μm × 0.25 μm and platelets with 1.7 μm × 1.7 μm × 0.13 μm sizes were formed respectively. The surfaces of the platelets in Fig. 2c are covered with much smaller particles. The particles prepared without and with Span 60 at pH 8.2 were nanosized and they were agglomerated to larger sizes as seen in Figs. 2e and 2f, respectively.

3.3 Particle Size Distribution

The particles prepared at pH 3.1 were flat in shape and their sizes were 2 ± 0.2 μm length and 1 ± 0.1 μm width and 100 ± 10 nm. Since they were in an agglomerated state their size was not measured by zetasizer. The particle size distribution of the powder obtained at pH 10.1 determined by zeta sizer (Fig. 3a) was bidisperse. The average size of 35.3% of the particles was 183 nm and 64.7% of the particles had 715 nm size. The width of the distribution curves was 62 and 244 nm, respectively. Since the particles had platelet shape and zetasizer assumes that they were spherical, the bidisperse distribution observed was due to flat particle shape. The lower particle size (183 nm) and the higher size (715 nm) should have corresponded to the thickness and length of the particles as seen in Fig. 3a.

The particle size distribution of the particles obtained at pH 8.2 was very narrow as seen in Fig. 3b. The particles of the powder prepared at pH 8.2 had 27 and 44 nm sizes for the cases without and with Span 60 respectively. The breadth of the distribution curve was 14 nm for both cases. The nano particles formed at pH 8.2 were in larger size when Span 60 was added as indicated by curve 1 and curve 2 in Fig. 3b.

3.4 Crystal Structure of the Precipitates

X-ray diffraction diagram of the precipitate prepared at 70 °C with Span 60 and reacted for 4 h at pH 3.7 is seen in Fig. 4a. XRD patterns of all the samples prepared at pH 3.7 were identical to this pattern. The peak positions and the relative intensities of the peaks indicated that the samples had the same x-ray diffraction diagram of $Cu_2(OH)_3NO_3$ according to the studies of Park and Kim [12] and Aguirre et al[8]. The samples had main reflections at 2 theta values of 12.7, 25.6, 33.48, 36.4, 39.6 for reflections of 001, 002, 120, 121, 202 planes as indicated in JCPDS card number 15-0014 for monoclinic crystals of $Cu_2(OH)_3NO_3$. There were no diffraction peaks related to $Cu(BO_2)_2$ and $CuBO_2$ shown in JCPDS cards 01-1472 and 28-1286, respectively in the X-ray diagrams of the precipitates obtained in the present study. The size of the crystals (B) perpendicular to 001 and 120 planes were in the range of 76 to 104 nm as determined from the breadth of the related diffraction peaks and by Scherrer Equation (Eq. (1)) and they were

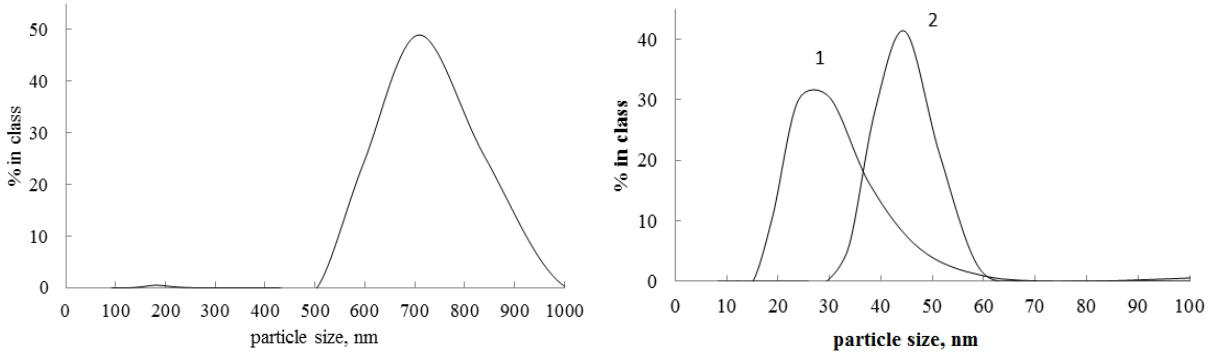

Fig. 3 Particle size distribution of powders obtained at (a) pH 10.1 (b) pH 8.2 without Span 60 (curve 1) and with Span 60 (curve 2).

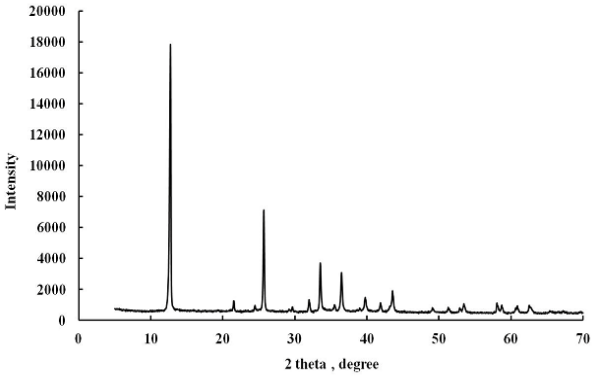

(a)

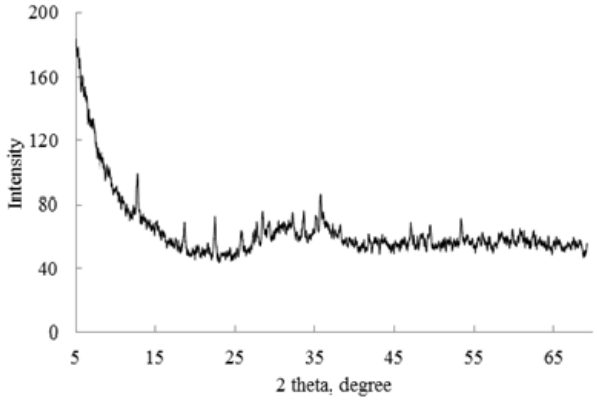

(b)

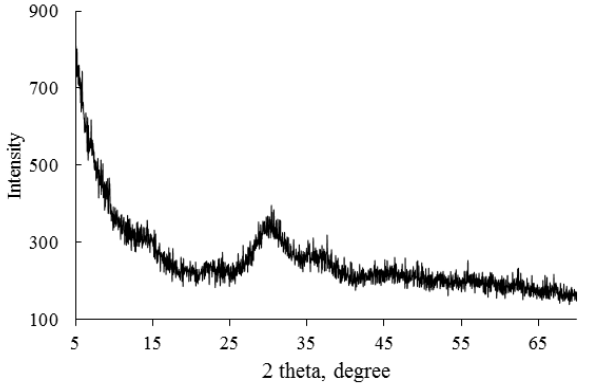

(c)

Fig. 4 X-ray diffraction of sample prepared (a). at 70 °C with Span 60 and reacted for 4h at pH 3.7, (b) at pH 10.1 without Span 60, (c) at pH 8.2 without Span 60.

were reported in Table 3.

$$B = K\lambda/L\cos\theta \quad (1)$$

where, K is constant taken as 0.9, λ is the wavelength of the X-rays, 0.146 nm for the present case, L is the breadth of the diffraction peak in radians at θ degree. However, the crystals were self-assembled to planar structures having 2 ± 0.2 μm length and 1 ± 0.1 μm width on the average as seen in Fig. 2.

Table 3 Size of crystals (nm) from 001 planes and 120 planes at at 2θ values of 12.7° and 33.48°, respectively for $Cu_2(OH)_3NO_3$ crystals present in the precipitate obtained prepared at pH 3.7 predicted by Scherrer equation.

Time (h)	Span 60 (%)	001 planes		120 planes	
		40 °C	70 °C	40 °C	70 °C
2	None	94	100	83	93
4	None	76	100	83	83
2	Present	80	80	98	83
4	Present	80	100	104	83

The X-ray diffraction diagram of powders obtained at pH 10.1 is seen in Fig. 4b. There are crystalline peaks overlapped with the broad amorphous scattering. There were diffraction peaks at 2θ values of 12.8°, 18.7°, 22.4°, 24.4°, 28.5°, 33.5°, 35.6°, 46.2°, 48.5°, 65.3°. These peaks were nearly identical with the peaks at 2θ values of 12.5°, 20.6°, 22.9°, 24.2°, 27.2°, 33.9°, 35.4°, 46.9°, 48.8°, 63.8° of $CuBO_2$ reported in JSPDS card number 28-1256. A phase isomorphous with $CuBO_2$ was present in the powder. $Cu_2[(BO(OH)_2](OH)_3$ also had peaks at 2θ values of 13.8°, 18.2°, 22.5°, 27.8°, 30.5°, 33.6°, 35.1°, 39.5°, 43.4°, 52.4°, 58.6° [14]. Since some of the peaks of $Cu_2[(BO(OH)_2](OH)_3$ were present in the X-ray diagram it could also be present in the powder.

The peaks related to $Cu(BO_2)_2$ should have been observed at 2θ values of 13.9°, 16.7°, 22.9°, 28.7°, 33.8°, 35.9°, 8.09°,41.7°, 46.7° as reported in JSPDS card number 01-472 for $Cu(BO_2)_2$. Due to the absence of these peaks , $Cu(BO_2)_2$ was not present.

X ray diffraction diagram of the powder obtained at 8.2 without Span 60 is seen in Fig. 4c. It is very similar to the one with Span 60. There are no sharp diffraction peaks. There were broad diffraction peaks being maximum at 2θ values of 5.0°, 9.4°, 30.6° and 37.6°. Due to the nanosize of the particles, even if they were crystalline, their diffraction peaks were broadened and overlapped with each other. Thus it was not possible to say which crystalline phase was present in the powder by examining its X-ray diffraction diagram.

3.5 Functional Groups in Precipitates

Typical FTIR spectra of the powders obtained at pH 3.7, 10.1 and 8.2 are seen in Fig. 5. FTIR spectrum of the sample produced at 70 °C without Span 60 for 4 h at pH 3.7 is the curve 1 in Fig. 5. All other samples prepared at pH 3.7 also exhibit the similar spectra with this sample. The peaks at 3,547 and 3,491 cm^{-1} belong isolated and hydrogen bonded OH stretching peaks. The peaks at 1,422 and 1,360 cm^{-1} are asymmetric and symmetric stretching peaks of O-NO_2 respectively. The peak at at 1,047 cm^{-1} is attributed to N-O stretching vibration of monodendate O-NO groups [9]. The peaks at 869, 767 and 669 are due to bending vibrations of Cu-OH groups with different hydrogen bonds. The IR spectrum of copper hydroxy nitrate prepared by previous investigators [8, 11] is very similar to those of the precipitates obtained by Method 1.

The infrared spectrum of the powder obtained at pH 8.2 without Span 60 is shown by the curve 3 in Fig. 5. There is a broad peak at 3,416 cm^{-1} which represented the vibrations of hydrogen bonded O-H group. Bending vibrations of H_2O is observed at 1,620 cm^{-1}. Asymmetric and symmetric stretching of the B(3)-O group was observed at 1,383 $cm^{-1}$and 977 cm^{-1}. At 1230 cm^{-1} in plane bending of B-OH is observed. Out of plane bending of B(3)-O gave a small peak at 684 cm^{-1}.

The FTIR spectrum of the product obtained at pH 8.2 is shown by the curve 2 in Fig. 5. The shoulder at 3,543 cm^{-1} belongs to isolated OH groups vibrations. The broad peak being maximum at 3,468 cm^{-1} is due to vibrations of hydrogen bonded OH groups. The OH bending vibration is observed at 1,620 cm^{-1}. The peaks observed at 1,417, 1,384 and 1,340 cm^{-1} are for the asymmetric stretching vibrations of B(3)-O group. The peak at 1,230 cm^{-1} is due to in plane bending of B-OH group. The peak at 667 cm^{-1} or for the out of plane bending vibrations of the B(3)-O [15, 16].

3.6 Thermal Characterization of the Precipitates

TG curve for the sample prepared at 70 °C with Span 60 and mixed for 2 h at pH 3.7 is the curve 1 in Fig. 6.

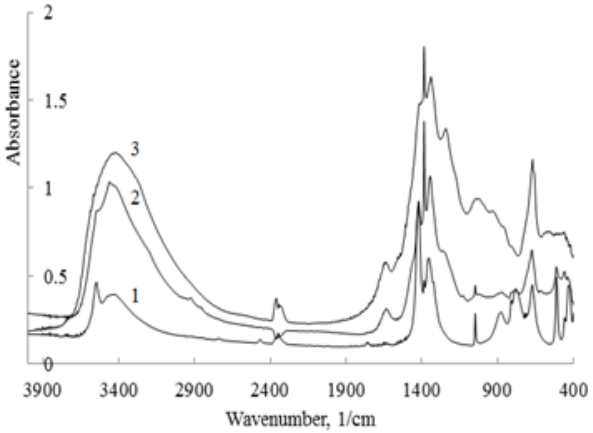

Fig. 5 FTIR spectra of samples prepared without Span 60 (1) at 70 °C reacted for 2 h at pH 3.7, (2) at 60 °C pH 10.2 and (3) at 25 °C and at pH 8.2.

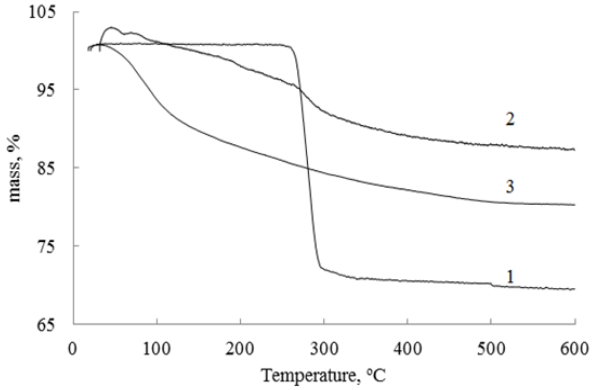

Fig. 6 TG curve of the samples prepared (1) at 70 °C with Span 60 and reacted for 2 h at pH 3.7, (2) at pH 10.2 and (3) at pH 8.2 without Span 60.

Other samples prepared at pH 3.7 had TG curves similar to this one. Since the FTIR spectroscopy indicated these powders had the same spectrum with copper hydroxy nitrate, their thermal decomposition behavior should be similar to that of copper hydroxy nitrate. The most commonly accepted mechanism for the thermal decomposition of copper hydroxyl nitrate is described by Eq. (2) [9].

$$Cu_2(OH)_3(NO)_3\,(s) \rightarrow 2CuO(s) + HNO_3(g) + H_2O(g) \quad (2)$$

De-hydroxylation and decomposition of the anion in the interlayer space should take place leading to the destruction of the layered structure during heating. The temperature of the thermal decomposition process of copper hydroxyl nitrate was reported to be 246 °C [9] which was very close to those of the precipitates obtained in the present study. The mass loss onset

temperatures of the all samples were between 237.7 and 248.7 °C as shown in Table S1. The remaining mass after thermal decomposition would be 66% considering the stoichiometry of the reaction in Eq. 2. The remained mass from the samples at 600 °C were in the range of 63.4% and 70.9% as indicated in Table S1. The higher values of remained mass than 66% indicated that there were other nonvolatile components such as a borate compound in the precipitates.

TG curves for precipitates prepared at pH 10.1 and 8.2 without Span 60 are shown by the curves 2 and 3 in Fig. 6. Their TG curves do not have a step change like the powders obtained at pH 3.7. The mass losses for these compounds are due to elimination of free water up to 100 °C and of bound water as OH groups above this temperature. There is a smooth mass loss down to 96% at 258 °C and it decreases at a faster rate down to 93 % at 295 °C and the remaining mass at 600 °C is 87% for the powder prepared at pH 10.1. It can be concluded the 13% mass loss was due to elimination of free and bound water from the sample. Since the powder prepared at pH 8.2 was only dried at 25 °C, it had a high value of free water content. As seen in the curve 3 in Fig. 6 there is a smooth mass loss down to 92% at 100 °C and the mass loss continues at a slower rate at higher temperatures. The remaining mass is 80% at 600 °C. In other words there are 8% free water and 12% bound water in this sample.

DSC curve of the sample prepared at 70 °C with Span 60 and mixed for 2 h at pH 3.7 is given by the curve 1 in Fig. 7. The DSC curves of the other samples prepared at pH 3.7 were also similar to this curve. As reported in Table S1 all the samples decomposed by an endothermic reaction and the heat of decomposition were between 640.2 and 996.8 J/g as determined from the area of the peak with 260 °C maximum. The curve 2 in Fig. 7 is for the sample prepared at pH 10.1. It does not show any sharp dehydration or decomposition peak. The curve 3 in Fig. 7 is for sample prepared at pH 8.2 and it has an endothermic peak being maximum around 77 °C. This peak corresponds to 8% mass loss observed in TG curves and it is related to desorption of free water from the sample.

3.7 The in Situ Drift FTIR Spectroscopy

The *in situ* drift FTIR spectroscopy study of the samples give information about the functional groups on the surface of the particles. In Fig. 8a, 8b and 8c *in situ* drift spectra of the samples during heating them from 25 °C to 600 °C at 2 °C/min heating rate are exhibited. The spectra taken during heating of the sample prepared at pH 3.7 showed the elimination of OH groups and NO_3^- ions by heating (Fig. 8a). The peaks related to OH groups at 3,520 cm^{-1} and 3,400 cm^{-1} and the peaks related to nitrate ions at 1,411 cm^{-1} and 1,327 cm^{-1} disappeared after thermal decomposition. A new peak appeared at 1,344 cm^{-1} at 300 °C which could be due to stretching vibrations of three coordinate boron, B(3)-O groups [15, 16]. This peak overlapped with the peaks of nitrate groups in unheated samples and it was clearly observed when nitrate groups were eliminated from the sample by heating.

The drift FTIR spectra of the powder prepared at pH 10.1 are seen in Fig. 8b. There is a broad peak at 3,400 cm^{-1} which decreases in intensity on heating. This shows hydrogen bonded OH groups are removed on heating the sample. The broad peak being maximum at 1,357 cm^{-1} which belong to B(3)-O vibrations did not

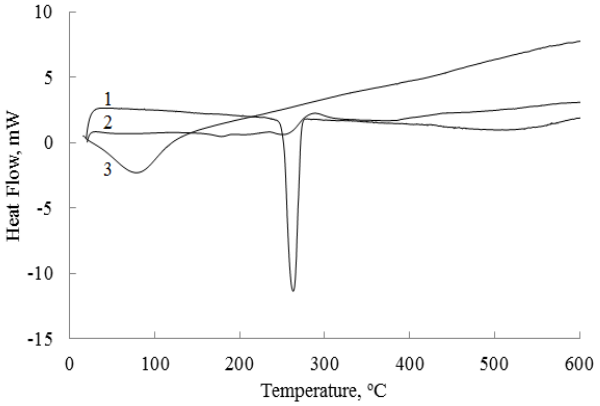

Fig. 7 DSC curve of samples prepared 1. at 70 °C with Span 60 and reacted for 2h at pH 3.7, 2. at pH 10.2, 3. at pH 8.2 without Span 60.

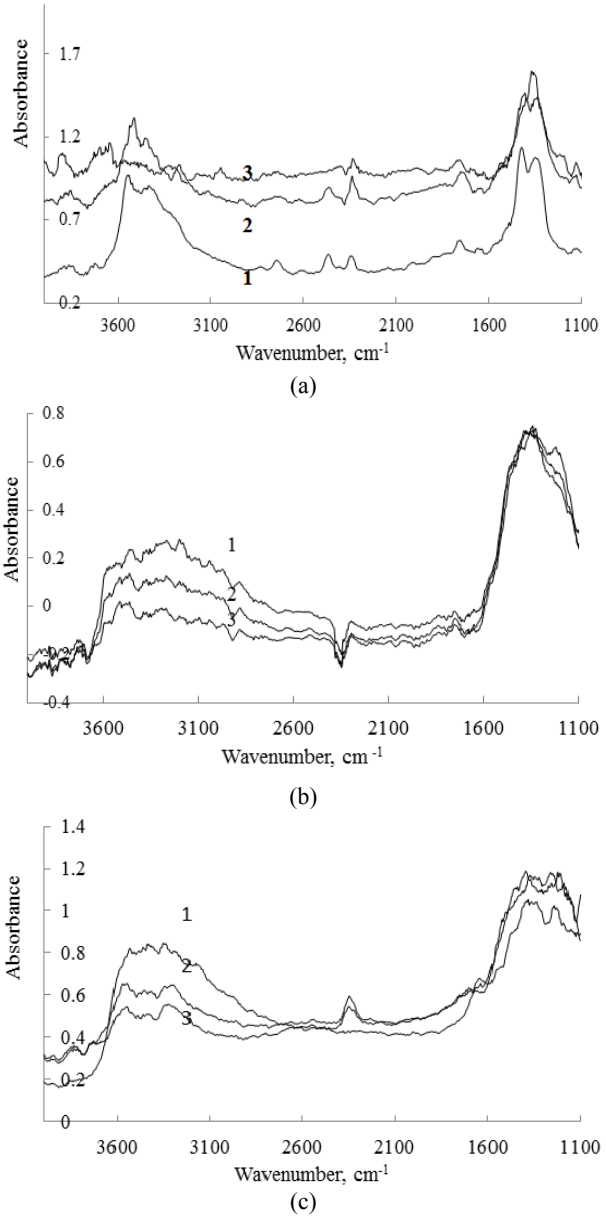

Fig. 8 Drift FTIR spectra of the samples produced (a) at 70 °C without Span 60 and reacted for 2h at pH 3.7, (b) pH 10.1, (c) at pH 8.2 without Span 60; at (1) 25 °C, (2) 200 °C, (3) 300 °C during dynamic heating experiment.

show any change in intensity on heating. A small shoulder was observed for B-OH stretching vibration at 1,210 cm^{-1} at 300-500 °C.

The drift FTIR spectra of the powder prepared at pH 8.2 without Span 60 are seen in Fig. 8c. The hydrogen bonded OH peak around 3,400 cm^{-1} decrease in intensity and B(3)-O asymmetric vibrations peaks at 1,350 cm^{-1} and B-OH stretching vibration at 1,213 cm^{-1} increase in intensity on heating.

The dehydration kinetics of the samples prepared at pH 3.7, pH 8.2 and pH 10.1 were examined by in situ FTIR spectroscopy. The change of the ratio of the absorbance of the hydrogen bonded OH peak at 3,400 cm^{-1} at any temperature (A) to the absorbance at 25 °C (A_o) versus temperature of the samples prepared at different pH values during dynamic heating in DRIFT cell are shown in Fig. 9. As seen in the figure the sample prepared at pH 3.7 dehydrated totally at 300 °C, and the samples prepared at pH 8.2 and at pH 10.1 continued to dehydration up to 500 °C. Dehydration rates of the sample prepared at pH 10.1 and pH 8.2 were close to each other indicating the stability of the OH groups in their structure were similar to each other. On the other hand, the sample prepared at pH 3.7 had OH groups which can be removed at a faster rate.

3.8 Chemical Composition of the Samples

The precipitates formed from sodium borate and copper nitrate solutions changed in composition depending on the pH, concentration and temperature of drying. Three main methods were used in the present study. Borax/copper ratio was 0.25, 0.87 and 1 for the methods 1, 2 and 3, respectively. The pH value of the mother liquors in equilibrium with the precipitates were 3.7, 10.1 and 8.1, respectively. Method 3 was for producing nano particles, thus dilute solutions and low

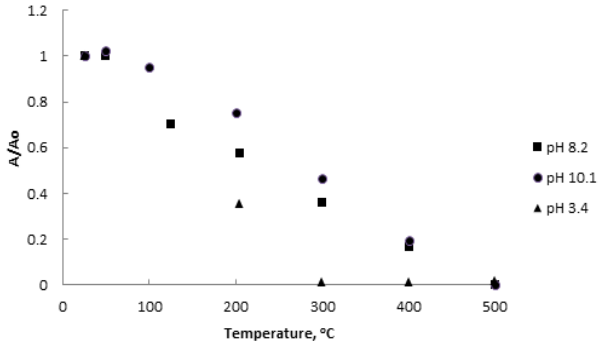

Fig. 9 A/A_o value at 3,400 cm^{-1} versus temperature for dynamic heating experiments for samples produced without Span 60 at 70 °C reacted for 2 h at pH 3.7, at pH 10.1 and pH 8.2.

temperature of mixing and drying were used to prevent crystal growth.

The chemical analysis of the samples indicated that they had Cu, O, N, B and H elements (Table 5). The reported Cu and B content in Table 4 were determined by ICP analysis and analytical titrations respectively. N and H content were obtained by CNHS analysis. EDX analysis indicated the presence of O element. However the reported oxygen content in Table 4 was calculated by mass balance since EDX analysis measured only approximate values for oxygen. The samples prepared under different conditions at pH 3.7 had on the average 47.7 ± 4.2% Cu, 2.6 ± 1.2% B, 5.9 ± 0.5% N, 1.2 ± 0.1% H and 34.1 ± 2.6% O elements. FTIR spectroscopy demonstrated that nitrogen existed as nitrate ions and H atoms were present as OH groups in the products. B element was present in trigonal coordination B(3)-O at 300 °C. X-ray diffraction analysis, TG and FTIR spectroscopy indicated the presence of $Cu_2(OH)_3NO_3$ in the precipitates. $Cu_2(OH)_3NO_3$ were obtained by adding aqueous sodium carbonate [8], aqueous ammonia [9] or solid $Mg(OH)_2$ [8] to aqueous copper nitrate solution. Neither copper carbonate [7] nor copper tetramine nitrate [9] were formed in these reactions. Only the OH ions introduced by basic solutions were consumed to form $Cu_2(OH)_3NO_3$. Similarly the precipitate having mainly the borate ions was not obtained at pH 3.7 in the present study. OH ions present in borax solution were consumed only and mainly $Cu_2(OH)_3NO_3$ was formed. The average chemical analysis indicated that for each mol of $Cu_2(OH)_3NO_3$ there were borate ions equivalent to 0.13 mol of $Cu(BO_2)_2$ in the samples. However, $Cu(BO_2)_2$ peaks were not present in the x-ray diffraction diagram. Some of the nitrate ions should have been replaced by the borate ions in infinite network of $Cu_2(OH)_3NO_3$ without changing its crystal structure. Since the partial substitution of nitrate ions of $Cu_2(OH)_3NO_3$ by benzoate ions [10], perchlorate ions [14] and hydroxydodecyl sulfate ions [9] were reported in previous studies, some of the nitrate ions should have been replaced by the borate ions in infinite network of $Cu_2(OH)_3NO_3$ without changing its crystal structure in the present study. Thus the precipitate obtained at pH 3.7 in the present study is called as copper hydroxy nitrate borate.

Table 4 Average elemental composition of the samples prepared under different conditions, Cu from ICP and B Mass % from analytical titrations, N and H from HCNS analysis, O from mass balance.

Method	pH	Elemental composition				
		Cu (%)	B (%)	N (%)	H (%)	O (%)
1	3.7	47.7 ± 4.2	2.6 ± 1.2	5.9 ± 0.5	1.2 ± 0.1	34.1 ± 2.6
2	10.1	54.8 ± 0.2	11.8 ± 0.2	1.2 ± 0.1	1.5 ± 0.1	30.7 ± 1.1
3	8.2	25.0 ± 0.2	5.5 ± 0.5	0.25 ± 0.1	2.2 ± 0.1	67.1 ± 0.3

Table 5 Copper and borate conversions of the processes and the mother liquor concentrations in equilibrium with the precipitates.

Method	Equilibrum pH	Conversion (%)		Mother liquor concentrations (mol/dm^3)	
		Cu	Borate	Cu	Borate
1	3.7	32	11	0.18	0.08
2	10.2	88	38	0.04	0.16
3	8.3	39	26	0.03	0.04

There are many parallel reactions that could occur when copper nitrate and borax solutions are mixed. Copper hydroxy nitrate is formed according to reaction shown by Eq. (3).

$$2Cu^{2+}(aq) + 3OH^{-}(aq) + NO_3^{-}(aq) \rightarrow Cu_2(OH)_3NO_3\ (s) \quad (3)$$

The pH of the reaction medium after addition of copper nitrate solution to borate solution was 3.7 in Method 1. This emphasized that neutralization of OH^- ions and additionally hydrolysis of water were also taken place releasing protons to the medium as shown in Eq. (4).

$$Cu^{2+}(aq) + 3H_2O(l) \rightarrow Cu(OH)_2(s) + 2H_3O^{+}(aq) \quad (4)$$

A solution rich in copper and borate ions having pH value 3.7 was remained after separation of the precipitate from the system. At this pH value it is expected that $B_4O_7^{-2}$ ions are transformed to H_3BO_3:

$$B_4O_7^{-2}(aq) + 2\ H_3O^+(aq) + 3H_2O(l) \rightarrow 4H_3BO_3(aq) \quad (5)$$

Boric acid is a weak acid having pK_a value of 9.14 for its first ionization reaction shown in Eq. (6):

$$B(OH)_3 + H_2O \rightarrow BO(OH)_2^- + H_3O^+ \quad (6)$$

$BO(OH)_2^-$ ions could replace the NO_3^- ions in copper hydroxy nitrate. The drift FTIR study also confirmed the presence of trigonal B(3)O groups at 300 °C in the precipitate. Thus the precipitate was named as copper hydroxy nitrate borate due to its composition. Even if there were unreacted Cu^{2+} cations and borate anions in the mother liquid in equilibrium with the precipitates, they did not react to form copper borate $xCuO.yB_2O_3.zH_2O$ using at pH 3.7 in the present study.

Excess OH^- ions added to the solution reacted with copper ions to form $Cu(OH)_2$ as shown in Eq. (7) and made the equilibrium pH 10.1 in Method 2.

$$Cu^{2+}\ (aq) + OH^-(aq) \rightarrow Cu(OH)_2(s) \quad (7)$$

The OH^- ions of the $Cu(OH)_2$ formed (Eq.7) should have been replaced by the borate ions present in the reaction medium. From the TG analysis and elemental composition the empirical formula of the powder obtained by this method was found as $Cu(BO_2)_{1.5}(OH)_{0.74}\cdot(H_2O)_{0.15}$. It also contained 0.11 mol NO_3^- ion per mol. A phase isomorphous with $CuBO_2$ was detected in the sample. $Cu_2[(BO(OH)_2](OH)_3$ was reported to have infinite chains of CuO_6 octahedra bound with each other with BO_3 groups [17]. Formation of $BO(OH)_2^-$ anions in the solution that will substitute OH^- ions in $Cu(OH)_2$ was observed [17].

$$2Cu(OH)_2 + BO(OH)_2^- \rightarrow Cu_2[(BO(OH)_2](OH)_3 + OH^- \quad (8)$$

Formation of $Cu_2[(BO(OH)_2](OH)_3$ would be possible according to Eq. (8).

From TG analysis and chemical composition nanoparticles having the empirical formula $Cu(BO_2)_{1.5}(H_2O)_6$ was obtained by mixing of dilute borate and copper solutions at pH 8.2 and drying at room temperature according to method 3. It contained 0.05 mol NO_3^- ions per formula weight. A copper borate with oxide formula of $2CuO\cdot3B_2O_3\cdot6H_2O$ was reported by Shvartz and Belousova [5] from boric acid, sodium hydroxide and copper sulfate. The oxide formula of the compound with the empirical formula $Cu(BO_2)_{1.5}(H_2O)_6$ is $2CuO\cdot3B_2O_3\cdot6H_2O$. Thus it can be concluded that $2CuO\cdot3B_2O_3\cdot6H_2O$ was formed under these conditions. However no information about the crystal structure was obtained from the diagram since the peaks were broadened and overlapped due to small size of the crystals.

3.9 Conversions of Copper and Boron Elements in the Processes

The percentage of output Cu in the precipitate to input Cu is defined as Cu conversion of the process. On the other hand the B conversion is defined as the percentage of output B in the precipitate to input B to the system. Table 6 reports the Cu and B conversions of the processes with different formulations. The conversions of the process with method 1 at pH 3.7 were in the range of 32% for Cu and 11% for B elements respectively for different operating conditions. The Cu conversion was 88% and B conversion was 38% for Method 2 at pH 10.1. Method 3 at pH 8.2 had 40% and 28% Cu and boron conversions, respectively. The equilibrium concentrations of the solutions are also reported in Table 5. The solution obtained with method 1 at pH 3.7 contained 0.18 $mol\cdot dm^{-3}$ Cu(II) ions and 0.08 $mol\cdot dm^{-3}$ borate ions. The equilibrium Cu(II) and borate concentration of the solution prepared at pH 10.2 with method 2 were 0.04 $mol\cdot dm^{-3}$ and 0.16 $mol\cdot dm^{-3}$, respectively. On the other hand the solution prepared at pH 8.2 had 0.03 and 0.04 $mol\cdot dm^{-3}$ Cu(II) and borate concentrations, respectively. All the solutions which are in equilibrium with the precipitates contained borate and copper (II) ions. Shvartz and Belousava [4] also reported metal borate mother liquors that can be used in wood or seed preserving applications as byproducts of zinc borate and copper borate formation from borax and metal sulphates [4].

3.10 The Precipitates as Lubricant Additives

Since a large number of papers have reported the anti-wear and friction reduction abilities of inorganic particles in oil, the lubrication behavior of precipitates was investigated using a four ball tester. The precipitates tested for lubricating additives had different chemical composition, morphology and particle size. The preparation conditions for tested precipitates were reported in materials and methods section. They were differentiated with their preparation pH since it was the most important variable.

The changes of the friction coefficients with time for different lubricating oils are seen in Fig. 10. The friction coefficients of the oil without any additive and the oil with 1% Span 60 were reported as 0.99 and 0.066 respectively in a previous study [18]. However, in the present study they were determined as 2.02 and 0.035. Span 60 was the main component of the additives in the lubricating oil that reduce the friction coefficient. The improvement of friction reduction ability of Span 60 can be explained by the formation of a continuous film similar to other surface active agents in concave of rubbing face which can decrease shearing stress [19]. When solid particles were added to mineral oil with Span 60, they will be dispersed homogeneously in lubricating oil since they would be covered with Span 60. The solid particles covered with the surfactant reduce the friction coefficient of the steel surfaces by rolling between them and by filling the imperfections on the surfaces [2] . The change of the friction coefficient depends on the chemical nature, geometry and the size of the solid particles. Submicron sized copper borate particles prepared at pH 10.1 reduced the friction coefficient from 0.035 to 0.025 as seen in Table 6. Nanoparticles prepared at pH 8.2 reduced the friction coefficient to a higher extent, down to 0.012. Compared to 8% reduction of friction coefficient by copper nano powders [3], the nano copper borate particles prepared at pH 8.2 in the present study were more efficient with 60% reduction in friction coefficient. In the literature it was explained

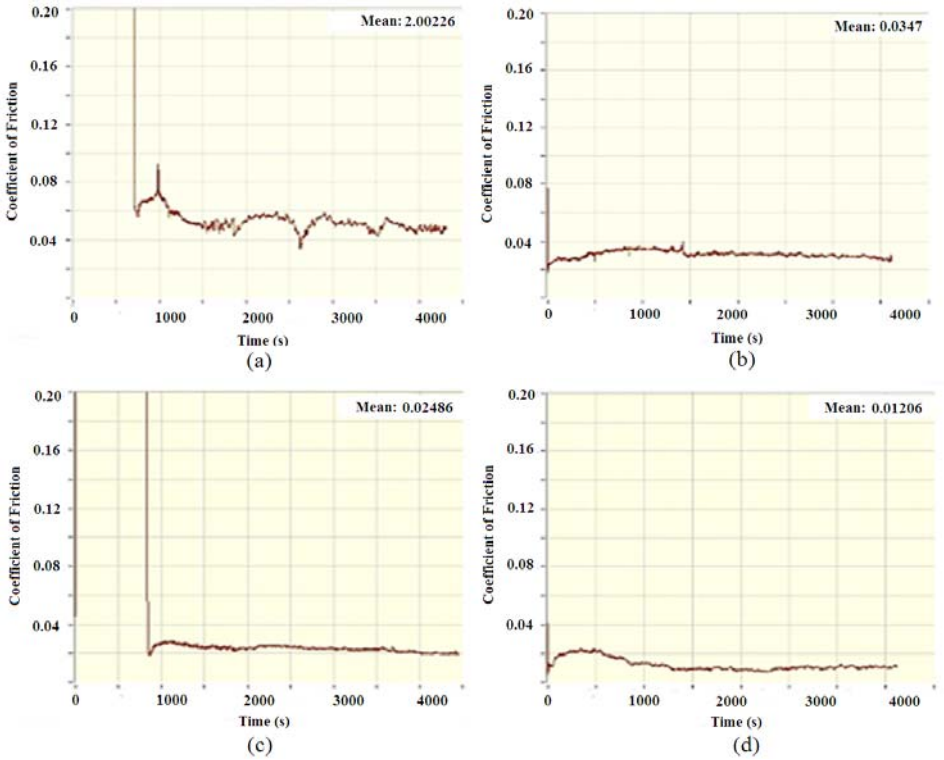

Fig. 10 Friction coefficient versus time for (a) spindle oil; (b) spindle oil with 1% Span 60; (c) spindle oil with 1% Span 60 and 1% copper borate (pH 10.1) and (d) spind le oil with 1% Span60 and 1% copper borate (pH 8.2).

Table 6 Wear scar diameter and friction coefficient of lubricants.

Additive	Average wear scar diameters of the three fixed balls (μm)	Wear scar thickness of the three fixed balls (μm)	Friction coefficient
None	806 ± 14	810	2.02
1% Span 60	491 ± 19	498	0.035
1% Span 60 + 1% Copper borate pH 10.1	622 ± 79	640	0.025
1% Span 60 + 1% Copper borate pH 8.2	532 ± 19	476	0.012

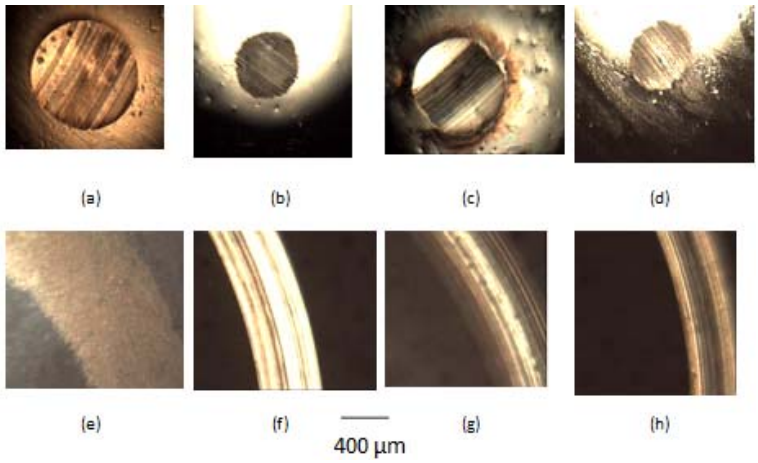

Fig. 11 Wear scar diameter of fixed and moving balls after testing with lubricating oils. Fixed ball of (a) mineral oil; (b) mineral oil with 1% Span 60; (c) mineral oil with 1% Span 60 and 1% copper borate (pH 10.1) and (d) spindle oil with 1% Span 60 and 1% copper borate (pH 8.2), moving ball of (a) mineral oil; (b) mineral oil with 1% Span 60; (c) mineral oil with 1% Span 60 and 1% copper borate (pH 10.1) and (d) mineral oil with 1% Span60 and 1% copper borate (pH 8.2).

that the hydrophobic copper borate particles covered with phosphate ester surfactant also had decreased the friction coefficient of lubricating oil more than the unmodified copper borate [2]. In the present study the nonionic surfactant Span 60 was added to make the copper borate particles hydrophobic and a very good result was obtained for the nanoparticles.

The wear scars of representative fixed and moving balls are seen in Fig. 11. The wear scar diameter on fixed ball and the thickness of the ring shaped scar for each oil were very close to each other as seen in Table 6. The wear scar diameter of the fixed ball was 806 μm and 494 μm for mineral oil and mineral oil with Span 60 as seen in Table 6. They were reported to be 1,402 μm, 639 μm in a previous study [18]. Both studies indicated the decrease of the wear scar diameter with Span 60 additive. The oil having Span 60 copper borate pH 10.1 had a larger wear scar diameter (622 μm) than that of the oil with only Span 60 (494 μm). On the other hand the wear scar diameter (532 μm) of the oil with Span 60 and nano copper borate particles prepared at pH 8.2 were higher than that of the oil with only Span 60. This indicated nano copper borate particles did not reduce the wear scar diameter of lubricating oil with span 60, but reduced the friction coefficient.

4. Conclusions

Particles nanosized only in thickness were obtained as the product of the precipitation process of copper nitrate and sodium borate solutions at pH 3.7 using Method 1. They were thermally stable up to 237 °C. They contained Cu, B, N, O and H elements. The precipitation process operated with low conversions with nearly 35.1%-47.9% for Cu and 7.0%-23.8% for B elements respectively for a solid precipitate. For each mol of $Cu_2(OH)_3NO_3$, 0.32 mols $Cu(BO_2)$ appears to be formed. However no crystal peaks related to $Cu(BO)_2$ was observed in the X-ray diagram of the product. Thus it was concluded that the borate ions replaced partially the nitrate ions in $Cu_2(OH)_3NO_3$ without changing its crystal structure. Thus the precipitate obtained at pH 3.7 was called as copper hydroxy nitrate borate.

Different products were formed pH 10.2 and 8.2 which can be represented by the empirical formulas Cu

$(BO_2)_{1.5}(OH)_{0.74}\cdot(H_2O)_{0.15}$ and $Cu(BO_2)_{1.5}(H_2O)_6$, respectively. Presence of a phase isomorphous with $CuBO_2$ or $Cu_2[(BO(OH)_2](OH)_3$ was observed at pH 10.2. While the The Cu conversion was 88% and 40% and the the B conversion was 38% and 28% for at pH 10.1 and 8.2, respectively.

For all three methods there were trigonal borate ions in the precipitates as indicated by transmission and drift FTIR spectroscopy. They all had hydrogen bonded OH groups which were removed by heating them to high temperatures. The products obtained at pH 10.1 and 8.2 also contained water molecules.

The precipitates obtained at pH 10.1 and 8.2 were tested as lubricant additives. When submicron precipitate prepared at pH 10.1 were added to lubricating oil with Span 60, the friction coefficient was reduced 28%. The nanoparticles prepared at pH 8.2 were more effective in reducing the friction coefficient. They reduced the friction coefficient by 65%. However wear scar diameters were increased compared to addition of only Span 60.

Acknowledgments

OPET FUCHS (Izmir Turkey) is acknowledged for four ball tests of the lubricants.

References

[1] S.Z. Hu, J.X. Dong, G.X. Chen, F. Lou, Preparation of nanometer copper borate with supercritical carbon dioxide drying, Powder Technology 102 (1999) 171.

[2] Y. Zheng, Z. Wang, Y. Tian, Y. Ou, S. Li, D. An, et al., Synthesis and performance of 1D and 2D Copper borate nano/microstructures with different morphologies, Colloid and Surfaces A: Physicochem. and Eng. Aspects. 349 (2009) 156.

[3] H.L. Yu, Y. Xu, P.J. Shi, B.S. Xu, X.L. Wang, Q. Liu, Tribological properties and lubricating mechanisms of Cu nanoparticles İn lubricant, Trans. Nonferrous Met. Soc. China 18 (2008) 636.

[4] E.M. Shvartz, R.G. Belousova, Synthesis of Zinc and copper borates in a single technological cycle, Russian Journal of Applied Chemistry 79 (2005) 893.

[5] E.M. Shvartz, R.G. Belousova, Formation of tricuprotetraborate $3CuO\cdot2B_2O_3\cdot6H_2O$ in aqueous solutions, Russian Journal of Applied Chemistry 79 (2006) 672.

[6] S.C. Neumair, R. Kaindl, R.D. Hoffmman, H. Huppertz, The New High-Pressure Borate Hydrate $Cu_3B_6O_{12}.H_2O$, Solid State Sciences 14 (2012) 229.

[7] E.J. Bushong, C.H. Yoder, The synthesis and characterization of rouartite, a copper hydroxy nitrate, An Integrated First-Year Laboratory Project Journal of Chemical Education 86 (2009) 80-81.

[8] J.M. Aguirre, A. Gutiérrez, O. Giraldo, Simple route for the synthesis of copper hydroxy salts, J. Braz. Chem. Soc. 22 (2011) 546.

[9] E. Kandare, G. Chigwada, D. Wang, C.A. Wilkie, J.M. Hossenlopp, Nanostructured layered copper hydroxy dodecyl sulfate: A potential fire retardant for poly(vinylester) (PVE) polm, Deg. And Stab. 91 (2006) 1781.

[10] T. Biswick, W. Jones, A. Pacula, E. Serwicka, Synthesis characterization and anion exchange properties of copper, magnesium, zinc and nickel hydroxy nitrates, Journal of Solid State Chemistry 179 (2006) 49.

[11] T. Biswick, W. Jones, A. Pacula, E. Serwicka, R. Cloots, Study of the morphology of copper hydroxynitrate nanoplatelets obtained by controlled double jet precipitation and urea hydrolysis, Journal of Crystal Growth 254 (2003) 176.

[12] S. Park, H.J. Kim, Unidirectionally aligned copper hydroxide crystalline nanorods from two-dimensional copper hydroxide nitrate, J. Am. Chem. Soc. 126 (2004) 14368-14369.

[13] D.C. Pereira, D. Lúcia, A. Faria, V.R.L. Constantino, Cu(II) hydroxy salts: Characterization of layered compounds by vibrational spectroscopy, J. Braz. Chem. Soc. 17 (2006) 1651.

[14] A.R. Kampf, G. Favreau, Jacquesdietrichite, $Cu_2BO(OH)_2(OH)_3$, a new mineral from tachgagalt mine, morocco: Descpription and crystal structure, Europan Journal of Minerology 16 (2004) 361.

[15] L. Zhihong, G. Bo, H. Mancheng, L. Shuni, X. Shuping, FT-IR and Raman spectroscopic analysis of hydrated cesium borates and their saturated aqueous solution, Specrochimica Acta Part A 59 (2003) 2741.

[16] L. Jun, X. Shupping, G. Shiyang, FT-IR and Raman spectroscopic study of hydrated borates, spectrochimica acta part A: Molecular and biomolecular spectroscopy 51 (1995) 519.

[17] H. Behm, C.H. Baerlocher, X-ray Rietveld Structure Determination of Trihydroxo[dihydroxo(oxo)borato] dicopper(II), $[Cu_2\{BO(OH)_2\}(OH)_3]$, Acta Cryst. C 41 (1985) 5-7.

[18] S.A. Savrik, D. Balkose, S. Ulku, Synthesis of zinc borate by inverse emulsiontechnique for lubrication, J. Therm. Anal. Calorim. 104 (2011) 605-612.

[19] T. Wasilewski, M.W. Sulek, Paraffin oil solutions of the mixture of sorbitan monolaurate-ethoxylated sorbitan monolaurate as lubricants, Wear 261 (2006) 230.